Investigation of a Solvent-cast Organogel to Form a Liquid-Gel Microinterface Array for Electrochemical Detection of Lysozyme

Bren Mark B. Felisilda, Eva Alvarez de Eulate, Damien W.M. Arrigan*

Nanochemistry Research Institute, Department of Chemistry, Curtin University, GPO Box U1987, Perth, Western Australia, 6845, Australia.

* Author for correspondence. Email d.arrigan@curtin.edu.au; phone +61-8-9266-9735.

Abstract

Ion transfer at aqueous-organogel interfaces enables the non-redox detection of ions and ionisable species by voltammetry. In this study, a non-thermal method for preparation of an organogel was employed and used for the detection of hen-egg-white-lysozyme (HEWL) via adsorptive stripping voltammetry at an array of aqueous-organogel microinterfaces. Tetrahydrofuran solvent casting was employed to prepare the organogel mixture, hence removing the need for heating of the solution to be gelled, as used in previous studies. Cyclic voltammetry of HEWL at the microinterface array revealed a broad adsorption process on the forward scan, at positive applied potentials, followed by a desorption peak at ca. 0.68 V, indicating the detection of HEWL in this region. Application of an adsorption step, where a constant optimized potential of 0.95 V was applied, followed by voltammetric detection provided for a linear response range of 0.02 – 0.84 µM and a detection limit of 0.030 µM for 300 s adsorption. The detection limit was further improved by utilizing differential pulse stripping voltammetry, resulting in detection limits of 0.017 µM, 0.014 µM, and 0.010 µM for adsorptive pre-concentration times of 60, 120 and 300 s, respectively, in unstirred solutions. These results are an improvement over other methods for the detection of HEWL at aqueous-organic interfaces and offers a basis for the label-free detection of protein.

Keywords

1. Introduction

Biomolecules, such as proteins, play a vital role in maintaining the functionalities of every activity within living species. Hence, understanding and detecting protein behaviour can be beneficial for a number of biomedical applications [1]. One of the commonly studied model proteins is lysozyme, a protein found in mammals that is responsible for the cleavage of an acetal group located in the polysaccharide walls of bacteria [2]. Composed mainly of 129 amino acids residues held together by cysteine disulphide bonds [3], it is usually available as hen-egg-white-lysozyme (HEWL) since it comprises 3.5% of egg white protein [4]. Its molecular weight is ca. 14,600 g mol^{-1} [2] and isoelectric point is 11.35, making it positively charged at physiological pH [5]. Aside from being a model protein analyte, the investigation of lysozyme was propelled by its use as an indicator for several diseases [6-8].

For the past 45 years, the study of electrochemistry at the interface between two immiscible electrolyte solutions (ITIES) has been rapidly increasing [9-11]. One of the main themes of research in this area in recent years has been the electrochemistry of proteins, since protein detection at the ITIES offers advantages for bioanalytical applications such as label-free detection, due to charge transfer processes at the ITIES, and amenability to miniaturization [12, 13]. Amongst several biomolecules of interest at the ITIES or μITIES, dopamine [14], heparin [15], and cytochrome C [16] have been investigated in addition to HEWL. Scanlon et al. examined the electrochemical behaviour of HEWL at the ITIES and showed its adsorption at both all-liquid ITIES and gellified μITIES. The proposed mechanism for its detection included adsorption of the cationic protein at the interface and the protein-facilitated transfer of the organic electrolyte anion across the interface, resulting in a protein-anion complex [17, 18]. This proposed complexation between the lysozyme and the organic electrolyte anion (hydrophobic) was demonstrated by Hartvig et al. [19] using an online mass spectrometry method to reveal this complexation. Subsequent mass spectrometry studies revealed partial unfolding of lysozyme following its electroadsorption at the aqueous-

2

55 organogel interface [20]. Similar detection mechanisms were suggested for other

56 biomacromolecules, including insulin [21] and haemoglobin [22, 23].

57   In terms of detection limits for HEWL at the ITIES, reports have been within the low

58 micromolar range, such as that based on background-subtracted cyclic voltammetry at a

59 µITIES array that detected 0.5 µM [17]. However, lower detection limits are required for protein

60 detection when applied in clinical diagnostics [24]. One common method that is utilized by

61 researchers to address such concerns for low detection limits is in the form of pre-

62 concentration. In voltammetric analysis, this entails pre-concentrating the analyte into or onto

63 the electrochemical interface before application of the voltammetric analysis. This is referred

64 to as stripping voltammetry and a recent review by Herzog and Beni [25] highlighted how this

65 technique has been applied to µITIES arrays. In particular, its application to exploiting protein

66 adsorption at the µITIES array has enabled lysozyme detection at 30 nM [26] as well as

67 haemoglobin at ~40 nM [27] and insulin at 10 nM [28]. In all such methods, however, the

68 organic phase was prepared using a high temperature process that involves pouring the hot

69 gel mixture into the micro-interface-forming membrane and allowing it to cool [17, 18, 26-29].

70 However, alternative methods for organogel preparation, such as the solvent-casting methods

71 widely used in potentiometric ion-selective electrode research [30, 31], may offer a more

72 convenient method for the preparation of the gelled organic phase.

73   The purpose of the work reported here was to examine whether the solvent-casting

74 organogel preparation method was a viable approach for the development of a gelled µITIES

75 array for protein detection. The combination of this method with adsorptive stripping

76 voltammetry and differential pulse voltammetry will be described in the following sections, with

77 a low detection limit of 10 nM achieved.

78

79

80 **2. Materials and Methods**

81   **2.1 Reagents**

82   All reagents were obtained from Sigma-Aldrich Australia Ltd. and were used as

83 received unless otherwise stated. The organic phase was prepared by dissolving

84 bis(triphenylphosphoranylidene) tetrakis(4-chlorophenyl)borate (BTPPA$^+$TPBCl$^-$, 10 mM) in

85 1,6-dichlorohexane (1,6-DCH). A volume (2.5 ml) of this electrolyte solution was then gelled

86 by the addition of 10% w/v low molecular weight poly(vinyl chloride) (PVC) [17, 32]. In order

87 to dissolve the PVC, a maximum equal volume (2.5 ml) of tetrahydrofuran (THF) was added

88 dropwise to the mixture, with continuous stirring over a *ca.* 15-20 min time. The resulting

89 solution was then set aside for 48 hours to evaporate excess solvent before being used [30].

90 The gel mixture was used for a maximum of a further 28 hours after this evaporation period.

91 The organic electrolyte salt (BTPPA$^+$TPBCl$^-$) was prepared by metathesis of

92 bis(triphenylphosphoranylidene) ammonium chloride (BTPPA$^+$ Cl$^-$) and potassium tetrakis(4-

93 chlorophenyl)borate (K$^+$TPBCl$^-$) following the published procedure [33]. The HEWL stock

94 solutions were prepared fresh in 10 mM HCl and then stored at 4°C. Similarly,

95 tetraethylammonium (TEA$^+$) chloride was dissolved in 10 mM HCl. All aqueous solutions used

96 were made with MilliQ water from a USF Purelab plus UV, having 18.2 MΩ*cm resistivity.

97   **2.2 Apparatus**

98   All electrochemical experiments were performed on an AUTOLAB PGSTAT302N

99 electrochemical station (Metrohm, The Netherlands) through a NOVA 1.9 software interface.

100 The µITIES array employed was defined by a micropore array silicon membrane, previously

101 described [34, 35]. The membrane employed in this study consisted of eight micropores in a

102 hexagonal arrangement, each having a diameter of 22 µm and a pore centre-to-pore centre

103 distance of 400 µm. These microporous silicon membranes were sealed onto the lower orifice

104 of a glass cylinder using silicone rubber (acetic acid curing Selley's glass silicone). The

105 solvent-cast organogel mixture was introduced into the silicon micropore arrays via the glass

106 cylinder with the aid of a pre-warmed glass Pasteur pipette. The set-up was then set aside for

4

107   at least one hour before use. When ready, the organic reference solution (composition: 10 mM

108   BTPPA$^+$Cl$^-$ in 10 mM LiCl) was then placed on top of the solvent-cast organic phase. The

109   solvent-cast organogel/silicon membrane assembly was then immersed into the aqueous

110   phase (10 mM HCl, HEWL in 10 mM HCl, and/or TEA$^+$ in 10 mM HCl) and voltammetric

111   experiments were implemented. Scheme 1 summarizes the electrochemical cell employed.

112   Each assembly of solvent-cast gel + silicon micropore array membrane was used for a

113   maximum of 1 day of experiments.

2.3 Electrochemical Measurements

115   A pair of Ag/AgCl electrodes were used for all measurements. The geometric area of

116   the microinterface array was 3.04 x 10^{-5} cm^2. Cyclic voltammetry (CV) and adsorptive stripping

117   voltammetry (AdSV) were carried out at a scan rate of 5 mV s^{-1}, unless noted otherwise.

118   Optimal parameters for differential pulse voltammetry were found to be 75 mV as the

119   modulation amplitude, 200 ms for the modulation time and 500 ms for the interval time, which

120   resulted in a scan rate of 10 mV s^{-1}. Other parameters such as protein concentration, applied

121   potential, and duration of the pre-concentration step were varied accordingly. In order to

122   compare all techniques utilized, all the calculated limits of detection were based on three times

123   the standard deviation of the blank (n=3) divided by the slope of the straight line. In the case

124   of the AdDPSV, when semi-logarithmic curves were observed, the slope of the straight line

125   was for the lower concentrations (0.02, 0.06 and 0.12 μM HEWL) only.

3. Results and Discussions

3.1 Cyclic Voltammetry

128   One approach to study the adsorption of a biomacromolecule at microITIES is via CV.

129   This can also be used to compare the voltammetric response for an ion transfer process in

130   the presence and absence of the target biomacromolecule [17, 36]. In this latter approach, the

131   CV shape for an ion transfer will be affected if the biomacromolecule is adsorbed at the

132   microITIES. Figure 1 shows CVs of HEWL at the solvent-cast aqueous-organogel

5

133   microinterface array. Figure 1a is the CV (grey line) obtained when 15 µM TEA$^+$ was present

134   in the aqueous phase. Figure 1a also shows the CV (dashed line) that was recorded when

135   only background electrolytes were present. The background electrolyte transfer across the

136   ITIES is indicated by the increase of current at the more positive potential end [17]. Meanwhile,

137   the CV in the presence of TEA$^+$ shows the typical CV shape at a micro-interface array formed

138   at silicon micropore array membranes, showing a steady-state voltammogram on the forward

139   (going to positive direction) scan, indicative of radial diffusion, and a peak-shaped

140   voltammogram on the reverse (going to negative direction) scan, indicative of linear diffusion

141   control. These mass transport phenomena dominate the ion transfer of TEA$^+$ at the microITIES

142   array and are concordant with previous reports in which the micropores were filled with gelled

143   organic phase [34, 35]. However, the case is different when HEWL is added to the aqueous

144   electrolyte phase. Figure 1b displays the CV (grey line) observed when 15 µM of HEWL was

145   present and Figure 1c shows the CV when 15 µM TEA$^+$ and 15 µM HEWL were present in the

146   aqueous phase. Overlayed in both is the background CV response (dashed line). The CV

147   obtained in the absence and presence of HEWL is distinguishable primarily by the reverse

148   scan peak, indicating that HEWL is detected. This peak can be attributed to the desorption of

149   HEWL from the interface, following its electroadsorption there during the forward scan.

150   Previous studies have discussed that the HEWL response at the liquid-liquid interface is

151   complex and is usually a mixture of HEWL adsorption at the interface and its participation in

152   the facilitated transfer of the background electrolyte anion from the organic to the aqueous

153   phase and the formation of a complex [17-19]. This complexity was exhibited as the presence

154   of HEWL changed the shape of the TEA$^+$ CV, as shown in Figure 1c. The steady-state

155   response of the TEA$^+$ transfer at the forward scan is less defined in comparison to the absence

156   of HEWL (Figure 1a). The intensity of the peak-shaped response of TEA$^+$ on the reverse scan

157   was also less-defined, as well as the existence of the additional peak due to the desorption of

158   HEWL. The peak for the TEA$^+$ transfer can be seen at ca. 0.62 V while that for desorption of

159   HEWL is at a more positive potential of ca. 0.68 V. The formation of an adsorbed protein layer

6

160 was shown by how the presence of HEWL transformed the shape of the expected steady-

161 state response for TEA$^+$ as it transfers from the aqueous into the organic phase. This was also

162 observed in a previous report [26] where a heat-treated gellification of the organic phase was

163 employed. The presence of HEWL has also affected the reverse scan peak as shown by the

164 slight shifting of the TEA$^+$ transfer peak potential and its decreased intensity. This can be

165 attributed to the presence of adsorbed HEWL that diminishes the area of the interface for TEA$^+$

166 transfer. In addition, the theoretical limiting current was also determined to characterize the

167 mass transport behaviour at the solvent-cast aqueous-organogel µITIES array. Using the

168 inlaid disc model [34], the limiting current was calculated to be 4.3 x 10^{-10} A, while using the

169 hemisphere model [37], it was found to be 6.7 x 10^{-10} A. When compared to the experimental

170 limiting current of 5.9 x 10^{-10} A for a 15 µM TEA$^+$ aqueous concentration, it is suggested that

171 the formed interface is in between that of an inlaid disc and hemispherical model.

172   CVs of increasing HEWL concentrations, in the range 5-25 µM, at the solvent-cast

173 aqueous-organogel µITIES array are illustrated in Figure 2. Despite the added HEWL

174 concentrations, a similar broad, indistinct rise in current for the forward sweep was observed

175 at every concentration. This can be related to the adsorption of HEWL at the interface, in

176 agreement with previous reports [18, 26]. However, the reverse scan was more revealing, as

177 the desorption peak increased with increasing HEWL concentration. This can be explained by

178 a desorption process following the complexation of the organic electrolyte anion with the

179 cationic protein. It was also shown in previous studies that multilayer formation [18, 20, 23]

180 occurs at the interface in the presence of increasing biomacromolecule concentrations, which

181 supports the idea that the reverse sweep current increases in proportion to the adsorbed

182 amount.

183   **3.2 Adsorptive Stripping Voltammetry**

184   The utilization of adsorptive stripping voltammetry (AdSV) for analytical detection

185 purposes at the µITIES has been studied for different model proteins [26-28]. AdSV involves

7

186   application of a constant potential, for a defined and controlled time, during which adsorption

187   occurs at the interface. This is then followed by the detection step, via a voltammetric scan to

188   lower potentials that desorbs the protein from the interface and produces a peak current that

189   is concentration- and adsorption time-dependent. In order to optimize the parameters for

190   HEWL adsorption at the solvent-cast aqueous-organogel microinterface array, the effect of

191   applied potential during the adsorption step was examined. The applied potential was held at

192   chosen values for various times, after which the potential was scanned to lower potentials so

193   as to desorb HEWL from the interface and yield a stripping voltammogram. The effect of

194   varying applied potentials on HEWL adsorption at the solvent-cast aqueous-organogel µITIES

195   is displayed in Figure 3. In consideration of the effect of the adsorption potential on the peak

196   current, the optimum potential chosen must not only maximise the stripping signal but also

197   minimise the background (electrolyte transfer) signal which occurs in the region of HEWL

198   adsorption. The best compromise was determined to be at 0.95 V for HEWL, in agreement

199   with the results for the heat-treated organogel [26]. Above this potential, the peak current starts

200   to display a shoulder and the increasing current may be mostly due to background electrolyte

201   transfer contributions.

202   In order to examine whether the peak on the AdSV scan was indeed

203   adsorption/desorption related, voltammograms were recorded at different scan rates, to test

204   whether linear behaviour between peak current and scan rate was present, as predicted for

205   an adsorption process by the equation:

206   $$i_p = \frac{z_i{}^2 F^2 \Gamma A \upsilon}{4RT}$$ (1)

207   where i_p is the peak current, z_i refers to the number charges each molecule transfers, F is

208   the Faraday constant, R is the universal gas constant, T is the temperature and A is the total

209   interfacial area. Figure 4 illustrates the recorded voltammograms following application of a

210   constant potential and constant time for protein adsorption. The inset displays the linear

8

211 relationship between the peak current and the scan rate, verifying that the peak is associated

212 with desorption from the interface. Using the temperature of 21 °C, together with the

213 assumption that the number of ions transferred per molecule is equal to the charge of the

214 protein, +17 [38], and that the formed interface follows that of an almost hemispherical model,

215 the surface coverage for a 0.5 μM HEWL concentration adsorbed for 60 s was obtained from

216 the slope of the line of the inset graph, giving the value of 2.5 pmol cm^{-2}, which is in good

217 agreement with previously reported value, 4 pmol cm^{-2} [26].

218 In addition, the effect of varying the adsorption time was investigated and the resulting

219 voltammograms are shown in Figure 5. Without any pre-concentration (0 s adsorption time),

220 no stripping peak was observed for an HEWL concentration of 0.5 μM. However, LSV following

221 adsorption times of more than 60 s produced stripping peaks and the peak current continued

222 to rise as adsorption time was increased. To ensure that there was no carryover of HEWL

223 between experiments, a blank analysis was performed between all voltammograms; no peaks

224 were evident on these blank analyses.

225 Furthermore, increasing concentrations of HEWL (0-1.0 μM) were examined under

226 different adsorption times of 60, 120 and 300 s. The idea was to see how solution

227 concentration and adsorption time can be utilized to control HEWL adsorption and to maximise

228 the detection signal (current). Figure 6 compares the AdSV obtained for (a) 60 s and (b) 300

229 s pre-concentration times at increasing (0 -1.0 μM) HEWL concentration. It can be seen that

230 the peak currents increased with adsorption time, indicating that longer adsorption times can

231 improve the sensitivity. This agrees with previous reports [26] on the kinetics of HEWL

232 adsorption at the μITIES, where it was suggested that long pre-concentration times were

233 required for saturation or equilibrium surface coverage. In terms of analytical performance,

234 higher slopes from increased peak currents indicate better sensitivity and so 300 s was used

235 to investigate the analytical characteristic for AdSV at the solvent-cast aqueous-organogel

236 μITIES array. Figure 7 shows the voltammograms obtained when increasing concentrations

9

237 of HEWL were added (0.02 – 0.84 μM) to the aqueous phase. Concentrations of 0.04 μM were

238 detected and the calculated limit of detection was 0.03 μM. This value agrees with a previous

239 report on a heat-treated aqueous-organogel μITIES array [26], but is magnitudes better than

240 the reported value of 0.5 μM for CV detection at a heat-treated aqueous-organogel μITIES

241 array [17], and even more so for other ITIES studies on HEWL [18].

242 **3.3 Adsorptive Differential Pulse Stripping Voltammetry**

243 With the aim to further improve the detection limit of HEWL at a solvent-cast aqueous-

244 organogel μITIES array, differential pulse voltammetry (DPV) was employed following the

245 HEWL adsorption, since DPV is a well-known method that achieves lower detection limits [39,

246 40] Similar to the major steps involved in AdSV, adsorptive differential pulse stripping

247 voltammetry (AdDPSV) employs a pre-concentration step followed by a voltammetric scan.

248 Background-subtraction was also utilized to further improve the sensitivity. Background

249 subtraction was performed by recording a blank experiment (0 μM HEWL) at the beginning of

250 the run. Then this blank response was subtracted from each of the pulse voltammetric

251 responses to HEWL subsequently recorded. Figure 8 shows the background-subtracted

252 voltammograms obtained at various HEWL concentrations. Voltammetric scans of a blank

253 experiment were performed in between runs to ensure that the solvent-cast aqueous-

254 organogel was clean prior to the next run [41]. The voltammograms corresponds to 60 s

255 (Figure 8a), 120 s (Figure 8b) adsorptive pre-concentration times. It is observed that as more

256 HEWL was added, the resulting desorption peak increased but also shifted to a less positive

257 potential. This produced a semi-logarithmic curve when plotted with HEWL concentration and

258 has been observed in other previous studies using pulse voltammetry [42, 43]. This may be

259 attributed to kinetic effects in the DPV detection mechanism, which is supported by the

260 observed broadening of peaks at the higher concentrations. Nevertheless, a linear increase

261 of peak current with concentration was observed at low concentrations, in the range of 0.02 to

262 0.12 μM HEWL.

10

263   Table 1 shows the summary of analytical characteristics of the various voltammetric

264   techniques employed in this study of a solvent-cast aqueous-organogel µITIES array for

265   HEWL detection. In order to compare all techniques utilized, all the calculated limits of

266   detection were based on three times the standard deviation of the blank (n=3) divided by the

267   slope of the straight line calibration plots. It is seen that from 4.5 µM for CV, the LOD has

268   improved to 0.030 µM for AdSV, mainly due to the additional 300 s pre-concentration step.

269   For the AdDPSV, which produced semi-logarithmic curves, the linearity observed on the lower

270   concentrations were used to determine the sensitivity of the calibration (n=3). Overall, longer

271   pre-concentration times for the AdDPSV has further enhanced the limit of detection from 0.017

272   µM with only 60 s pre-concentration time, to 0.014 µM after 120 s pre-concentration time, and

273   to 0.010 µM following 300 s pre-concentration time. However, the desorption peaks for the

274   300 s pre-concentration time were already broadened. In terms of precision, the relative

275   standard deviation was 3.8% for CV (n=4, 15 µM HEWL), 7.6% for AdSV (n=10, 0.30 µM

276   HEWL) at 300 s pre-concentration, while it was 3.2%, 7.4% and 5.8% (n=6, 0.02 µM HEWL)

277   for AdDPSV at 60, 120 and 300 s pre-concentration times, respectively.

278   Furthermore, a comparison of the heat-treated organogel versus the solvent-casting

279   organogel was done using AdDPSV with 400 s pre-concentration time. The results (not shown)

280   produced similar responses. As a result, the limit of detection and enhanced sensitivity are

281   attributed to the detection method used that combines the benefits of pre-concentration,

282   stripping voltammetry and differential pulse voltammetry.

283

284   4. Conclusions

285   Solvent-casting of PVC with THF was investigated as an alternative method to gel the

286   organic phase in the formation of a µITIES array for protein detection. The behaviour was

287   examined by cyclic voltammetry, adsorptive stripping voltammetry and adsorptive differential

288   pulse stripping voltammetry for its application to HEWL detection. CV results indicate that

289   HEWL is identified with a distinct peak on the reverse scan at ca. 0.68 V. Investigation of the

290   optimal adsorption potential for HEWL at this type of organogel shows that maximum protein

291   adsorption happens at a positive potential just below the potential range where background

292   electrolytes are transferred. With a pre-concentration time of 300 s for AdSV, a detection limit

293   of 0.03 µM was achieved. Differential pulse voltammetry was also utilized to further improve

294   the limit of detection for this solvent-cast aqueous-organogel system. The use of AdDPSV

295   enabled the same (0.017 µM) detection limit with only 60 s pre-concentration and still better

296   limits were obtained following 120 s (0.014 µM) and 300 s (0.010 µM) pre-concentration. This

297   work further supports the capacity of the use of electrochemistry at the µITIES array as a label-

298   free bioanalytical tool. However, studies on selectivity and sample matrix effects remain as

299   challenges currently being addressed.

Acknowledgement

References

[1] D.L. Nelson, A.L. Lehninger, M.M. Cox, Lehninger Principles of Biochemistry, Macmillan, New York, 2008.

[2] D.J. Vocadlo, G.J. Davies, R. Laine, S.G. Withers, Catalysis by hen egg-white lysozyme proceeds via a covalent intermediate, Nature, 412 (2001) 835-838.

[3] R.E. Canfield, A.K. Liu, The disulfide bonds of egg white lysozyme (muramidase), Journal of Biological Chemistry, 240 (1965) 1997-2002.

[4] K.L. Hoober, S.L. Sheasley, H.F. Gilbert, C. Thorpe, Sulfhydryl Oxidase from Egg White: A Facile Catalyst for Disulfide Bond Formation in Proteins and Peptides, Journal of Biological Chemistry, 274 (1999) 22147-22150.

315 [5] C.C. Blake, D.F. Koenig, G.A. Mair, A.C. North, D.C. Phillips, V.R. Sarma, Structure of hen

316 egg-white lysozyme. A three-dimensional Fourier synthesis at 2 Angstrom resolution, Nature,

317 (1965) 757-761.

318 [6] C. Serra, F. Vizoso, L. Alonso, J.C. Rodríguez, L.O. González, M. Fernández, M.L.

319 Lamelas, L.M. Sánchez, J.L. García-Muñiz, A. Baltasar, Expression and prognostic

320 significance of lysozyme in male breast cancer, Breast Cancer Res, 4 (2002) R16.

321 [7] E. Tahara, H. Ito, F. Shimamoto, T. Iwamoto, K. Nakagami, H. Niimoto, Lysozyme in human

322 gastric carcinoma: a retrospective immunohistochemical study, Histopathology, 6 (1982) 409-

323 421.

324 [8] O.P. Mishra, P. Batra, Z. Ali, S. Anupurba, B.K. Das, Cerebrospinal fluid lysozyme level for

325 the diagnosis of tuberculous meningitis in children, Journal of tropical pediatrics, 49 (2003)

326 13-16.

327 [9] P. Vanysek, L. Basaez Ramirez, Interface between two immiscible liquid electrolytes: a

328 review, Journal of the Chilean Chemical Society, 53 (2008) 1455-1463.

329 [10] H.H. Girault, Electrochemistry at liquid–liquid interfaces, in: A.J. Bard, C.G. Zoski (Eds.)

330 Electroanalytical Chemistry: A Series of Advances, CRC Press: Taylor & Francis, Boca Raton,

331 FL, 2010, pp. 1.

332 [11] Z. Samec, Electrochemistry at the interface between two immiscible electrolyte solutions

333 (IUPAC Technical Report), Pure and Applied Chemistry, 76 (2004) 2147-2180.

334 [12] D.W.M. Arrigan, Voltammetry of proteins at liquid–liquid interfaces, Annual Reports

335 Section" C"(Physical Chemistry), 109 (2013) 167-188.

336 [13] G. Herzog, Recent developments in electrochemistry at the interface between two

337 immiscible electrolyte solutions for ion sensing, Analyst, 140 (2015) 3888-3896.

338 [14] J.A. Ribeiro, I.M. Miranda, F. Silva, C.M. Pereira, Electrochemical study of dopamine and

339 noradrenaline at the water/1, 6-dichlorohexane interface, Physical Chemistry Chemical

340 Physics, 12 (2010) 15190-15194.

341 [15] S. Amemiya, Y. Kim, R. Ishimatsu, B. Kabagambe, Electrochemical heparin sensing at

342 liquid/liquid interfaces and polymeric membranes, Anal Bioanal Chem, 399 (2011) 571-579.

343 [16] T. Osakai, Y. Yuguchi, E. Gohara, H. Katano, Direct label-free electrochemical detection

344 of proteins using the polarized oil/water interface, Langmuir, 26 (2010) 11530-11537.

345 [17] M.D. Scanlon, J. Strutwolf, D.W.M. Arrigan, Voltammetric behaviour of biological

346 macromolecules at arrays of aqueous|organogel micro-interfaces, Physical Chemistry

347 Chemical Physics, 12 (2010) 10040-10047.

348 [18] M.D. Scanlon, E. Jennings, D.W.M. Arrigan, Electrochemical behaviour of hen-egg-white

349 lysozyme at the polarised water/1, 2-dichloroethane interface, Physical Chemistry Chemical

350 Physics, 11 (2009) 2272-2280.

351 [19] R.A. Hartvig, M.A. Méndez, M.v.d. Weert, L. Jorgensen, J. Østergaard, H.H. Girault, H.

352 Jensen, Interfacial Complexes between a Protein and Lipophilic Ions at an Oil− Water

353 Interface, Analytical Chemistry, 82 (2010) 7699-7705.

354 [20] E. Alvarez de Eulate, L. Qiao, M.D. Scanlon, H.H. Girault, D.W.M. Arrigan, Fingerprinting

355 the tertiary structure of electroadsorbed lysozyme at soft interfaces by electrostatic spray

356 ionization mass spectrometry, Chemical Communications, 50 (2014) 11829-11832.

357 [21] F. Kivlehan, Y.H. Lanyon, D.W.M. Arrigan, Electrochemical Study of Insulin at the

358 Polarized Liquid− Liquid Interface, Langmuir, 24 (2008) 9876-9882.

359 [22] G. Herzog, V. Kam, D.W.M. Arrigan, Electrochemical behaviour of haemoglobin at the

360 liquid/liquid interface, Electrochimica Acta, 53 (2008) 7204-7209.

361 [23] G. Herzog, W. Moujahid, J. Strutwolf, D.W.M. Arrigan, Interactions of proteins with small

362 ionised molecules: electrochemical adsorption and facilitated ion transfer voltammetry of

363 haemoglobin at the liquid| liquid interface, Analyst, 134 (2009) 1608-1613.

364 [24] N.L. Rosi, C.A. Mirkin, Nanostructures in biodiagnostics, Chemical Reviews, 105 (2005)

365 1547-1562.

366 [25] G. Herzog, V. Beni, Stripping voltammetry at micro-interface arrays: A review, Analytica

367 Chimica Acta, 769 (2013) 10-21.

368   [26] E. Alvarez de Eulate, D.W.M. Arrigan, Adsorptive stripping voltammetry of hen-egg-white-

369   lysozyme via adsorption–desorption at an array of liquid–liquid microinterfaces, Analytical

370   Chemistry, 84 (2012) 2505-2511.

371   [27] E. Alvarez de Eulate, L. Serls, D.W.M. Arrigan, Detection of haemoglobin using an

372   adsorption approach at a liquid–liquid microinterface array, Anal Bioanal Chem, 405 (2013)

373   3801-3806.

374   [28] S. O'Sullivan, E. Alvarez de Eulate, Y.H. Yuen, E. Helmerhorst, D.W.M. Arrigan, Stripping

375   voltammetric detection of insulin at liquid-liquid microinterfaces in the presence of bovine

376   albumin, Analyst, 138 (2013) 6192-6196.

377   [29] M.D. Scanlon, G. Herzog, D.W.M. Arrigan, Electrochemical Detection of Oligopeptides at

378   Silicon-Fabricated Micro-Liquid|Liquid Interfaces, Analytical Chemistry, 80 (2008) 5743-5749.

379   [30] G.J. Moody, Role of Polymeric Materials in the Fabrication of Ion-Selective Electrodes

380   and Biosensors, in: P.G. Edelman, J. Wang (Eds.) Biosensors and Chemical Sensors, in ACS

381   Symposium Series, American Chemical Society, Washington, 1992, pp. 99-110.

382   [31] G.J. Moody, J.D.R. Thomas, Poly(Vinyl Chloride) Matrix Membrane Ion-Selective

383   Electrodes, in: H. Freiser (Ed.) Ion-Selective Electrodes in Analytical Chemistry, Springer US,

384   New York, 1978, pp. 287-309.

385   [32] T. Osakai, T. Kakutani, M. Senda, Ion-transfer voltammetry and amperometric chemical

386   sensors, Journal of the Electrochemical Society, 134 (1987) C520-C520.

387   [33] H.J. Lee, P.D. Beattie, B.J. Seddon, M.D. Osborne, H.H. Girault, Amperometric ion

388   sensors based on laser-patterned composite polymer membranes, Journal of Electroanalytical

389   Chemistry, 440 (1997) 73-82.

390   [34] R. Zazpe, C. Hibert, J. O'Brien, Y.H. Lanyon, D.W.M. Arrigan, Ion-transfer voltammetry at

391   silicon membrane-based arrays of micro-liquid–liquid interfaces, Lab on a Chip, 7 (2007) 1732-

392   1737.

393 [35] J. Strutwolf, M.D. Scanlon, D.W.M. Arrigan, Electrochemical ion transfer across

394 liquid/liquid interfaces confined within solid-state micropore arrays–simulations and

395 experiments, Analyst, 134 (2009) 148-158.

396 [36] A. Berduque, M.D. Scanlon, C.J. Collins, D.W.M. Arrigan, Electrochemistry of non-redox-

397 active poly (propylenimine) and poly (amidoamine) dendrimers at liquid-liquid interfaces,

398 Langmuir, 23 (2007) 7356-7364.

399 [37] D.W.M. Arrigan, Nanoelectrodes, nanoelectrode arrays and their applications, Analyst,

400 129 (2004) 1157-1165.

401 [38] S. Kuramitsu, K. Hamaguchi, Analysis of the acid-base titration curve of hen lysozyme,

402 Journal of Biochemistry, 87 (1980) 1215-1219.

403 [39] J. Wang, Electroanalytical Techniques in Clinical Chemistry and Laboratory Medicine,

404 John Wiley & Sons, New Jersey, 1988.

405 [40] J. Wang, Analytical Electrochemistry, John Wiley & Sons, Hoboken, New Jersey, 2006.

406 [41] C.J. Collins, C. Lyons, J. Strutwolf, D.W.M. Arrigan, Serum-protein effects on the detection

407 of the β-blocker propranolol by ion-transfer voltammetry at a micro-ITIES array, Talanta, 80

408 (2010) 1993-1998.

409 [42] A. Berduque, R. Zazpe, D.W.M. Arrigan, Electrochemical detection of dopamine using

410 arrays of liquid–liquid micro-interfaces created within micromachined silicon membranes,

411 Analytica Chimica Acta, 611 (2008) 156-162.

412 [43] D. Zhan, S. Mao, Q. Zhao, Z. Chen, H. Hu, P. Jing, M. Zhang, Z. Zhu, Y. Shao,

413 Electrochemical investigation of dopamine at the water/1, 2-dichloroethane interface,

414 Analytical Chemistry, 76 (2004) 4128-4136.

415

416

Figure & Scheme captions

Scheme 1. Schematic representation of the electrochemical cell employed. *x* represents the various HEWL concentrations used in the study.

Figure 1. Cyclic voltammograms observed with the solvent-cast aqueous-organogel μITIES array (Scheme 1) in the absence and presence of TEA$^+$ and HEWL in the aqueous phase: a) 15 μM TEA$^+$; b) 15 μM HEWL and c) 15 μM TEA$^+$ + 15 μM HEWL. The blank experiment is shown as the dashed line. Scan rate: 5 mV s^{-1}.

Figure 2. Cyclic voltammograms observed with the solvent-cast aqueous-organogel μITIES array (Scheme 1) in the presence of increasing concentrations of HEWL, as indicated by the arrow direction (5, 10, 15, 20 and 25 μM), in the aqueous phase. Scan rate: 5 mV s^{-1}.

Figure 3. Plot showing the effect on the peak current of varying the interfacial potential on the adsorption step. Aqueous phase contains: 10 mM HCl + 10 μM HEWL. Adsorption time was 60 s, without stirring. The solvent-cast organogel was used as the organic phase (Scheme 1). Scan rate: 5 mV s^{-1}.

Figure 4. AdSV of 0.5 μM HEWL + 10 mM HCl at various scan rates: 5 mV s^{-1} (black bold line) to 60 mV s^{-1} (black dotted line). Inset shows plot of peak current against scan rate. The solvent-cast organogel was used as the organic phase (Scheme 1). Pre-concentration time and potential were 60 s and 0.950 V respectively.

Figure 5. AdSV of 0.5 μM HEWL + 10 mM HCl at various pre-concentration times from 5 (black bold line) to 1800 (grey bold line) s. The solvent-cast organogel was used as the organic phase (Scheme 1). Scan rate: 5 mV s^{-1}.

Figure 6. AdSV of various HEWL concentration for different adsorption times: (a) 60 s and (b) 300 s at an applied potential of 0.950 V. Aqueous phases contain (0 – 1.0) μM HEWL in 10 mM HCl. The solvent-cast organogel was used as the organic phase (Scheme 1). Scan rate: 5 mV s^{-1}.

442   **Figure 7.** AdSV of increasing aqueous phase HEWL concentrations, as indicated by the

443   direction of the arrow (0.02 to 0.84 µM) at the solvent-cast aqueous-organogel µITIES

444   (Scheme 1). The adsorption time and potential were 300 s and 0.950 V respectively. Scan

445   rate: 5 mV s^{-1}.

446   **Figure 8.** AdDPSV of HEWL (0.02 to 0.60 µM, increasing as directed by the arrow direction)

447   for a) 60 s, b) 120 s, pre-concentration times prior to voltammetric desorption. Solutions

448   contained increasing (0.02 - 0.60 µM) HEWL + 10 mM HCl in the aqueous phase (Scheme 1).

449

450

451

452

453

454 **Scheme & Figures**

455

456 **Scheme 1**

| Ag | AgCl | x μM HEWL in 10 mM HCl | 10 mM BTPPA⁺ TPBCl⁻ in solvent-cast (THF) gel with 1,6-DCH | 10 mM BTPPA⁺Cl⁻ in 10 mM LiCl | AgCl | Ag |

457

458

459

460

19

461   **Figure 1**

462

463

464
465

466
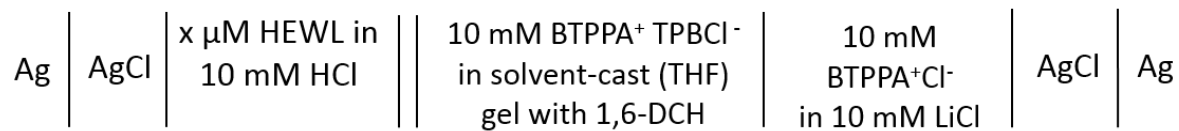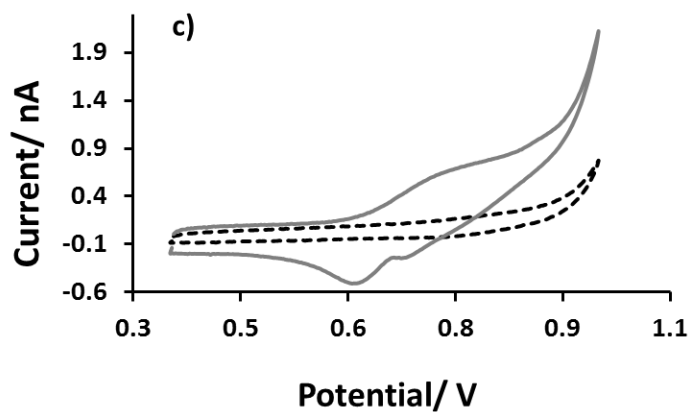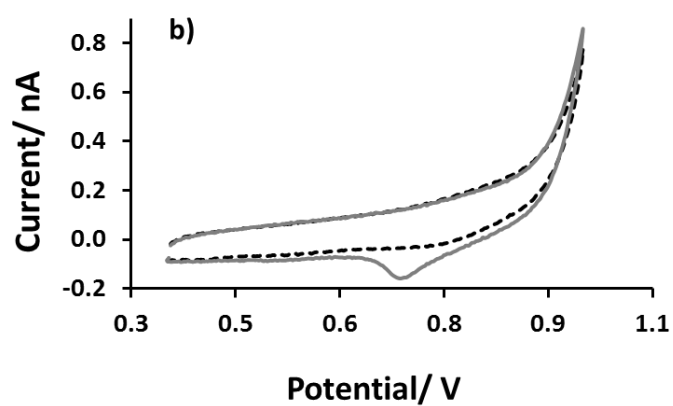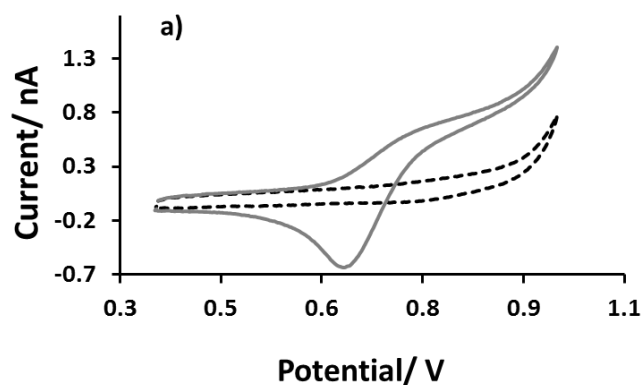
467 **Figure 2**

468

469
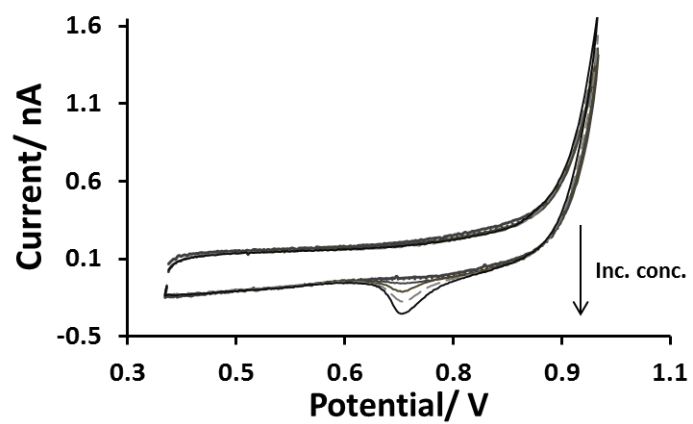
470

471

472   **Figure 3**
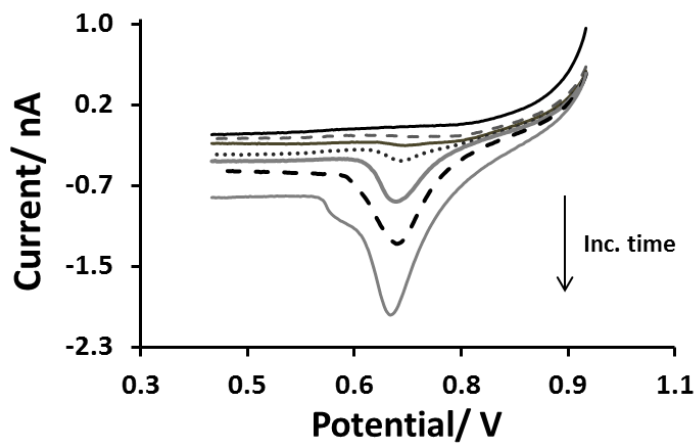
473
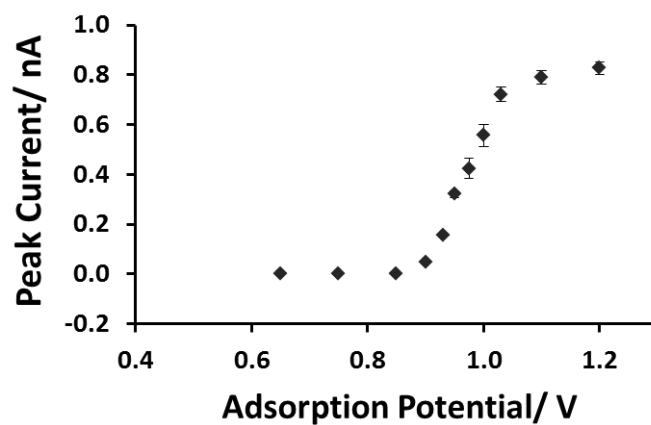
474

475

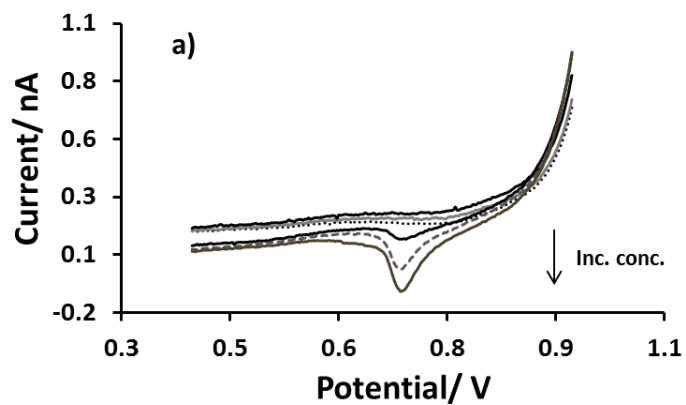476 **Figure 4**

477

478
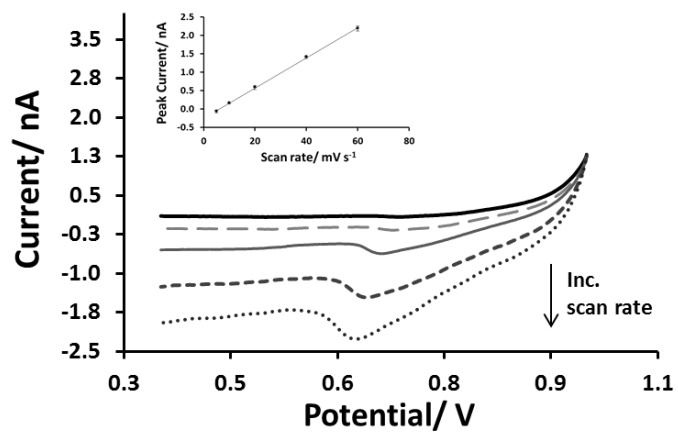
479

480

481

482 **Figure 5**

483

484

485

486

487

488 **Figure 6**
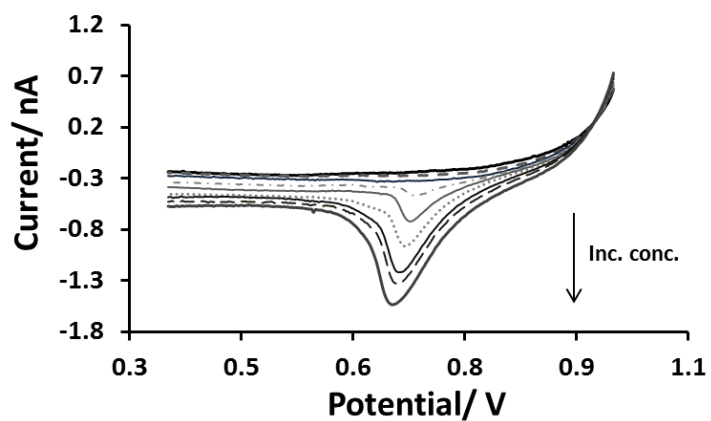
489
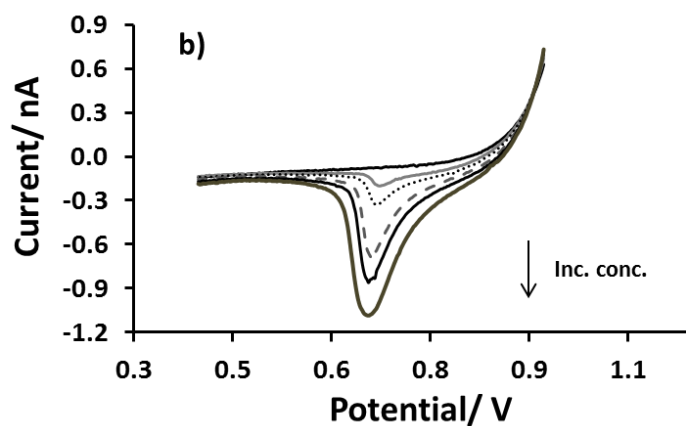
490

491
492

493

494

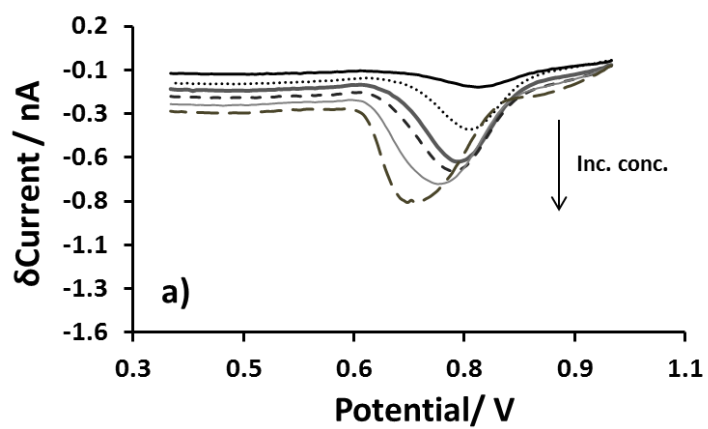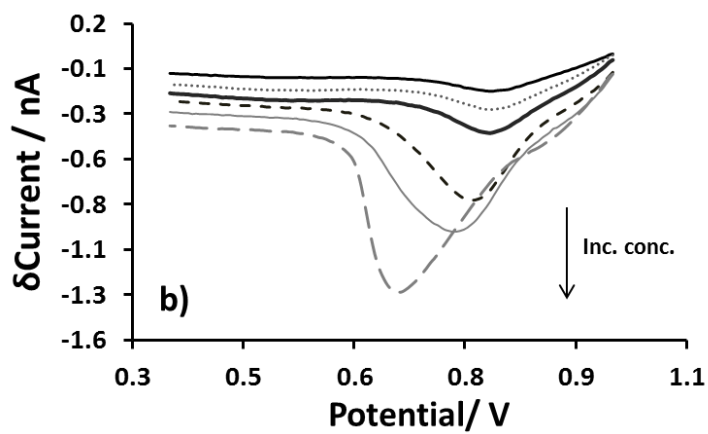495   **Figure 7**

496

497

498

499   **Figure 8**

500

501

502

503

504

505

506

507

508 **Table 1.** Summary of analytical performance of the solvent-casted organogel
509 microarray for different voltammetric techniques used.

Detection Method	Preconcentration time / s	Sensitivity (calibration graph) / nA μM^{-1}	Number † of Points (n)	Limit of Detection (LOD) / μM	Concentration Range / μM	Correlation Coefficient (R)
CV	0	0.0109	6	4.5	5-25	0.985
AdSV	300	1.62	9	0.030	0.02-0.84	0.993
AdDPSV	60	4.57	7 (3)	0.017	0.02-0.60	0.990
AdDPSV	120	3.55	7 (3)	0.014	0.02-0.60	0.992
AdDPSV	300	3.42	7 (3)	0.010	0.02-0.60	0.998

510 †Corresponds to the number of HEWL concentrations used providing the data points fitted for the linear regression. Since
511 AdDPSV resulted in semi-logarithmic curves, the slope across the lowest three (3) concentrations was used.
512

513